CHAPTER 87

SWASH OSCILLATION AND RESULTING SEDIMENT MOVEMENT

by Nobuhisa Kobayashi¹, Michael S. Strzelecki² and Andojo Wurjanto³

<u>ABSTRACT</u>: A numerical model for predicting the swash oscillation on a beach is described and compared with field data on wave setup and swash statistics on a moderately steep beach with a nearshore bar.

INTRODUCTION

The swash zone on a beach forms the boundary zone between the surf zone and backshore. Wave run-up is the upper limit of wave uprush and determines the landward boundary of the area affected by wave action. Few studies have been performed for the hydrodynamics and resulting sediment movement in the swash zone probably because existing hydrodynamic models such as those proposed by Battjes and Stive (1985) and Svendsen et al. (1987) do not account for the variations of hydrodynamic quantities over a wave period which are essential in the swash zone. A quantitative understanding of sediment transport in the swash zone is required for better establishing the landward boundary condition for existing cross-shore sediment transport models such as that proposed by Stive (1986) and De Vriend and Stive (1987). Furthermore, the temporal variation of the horizontal fluid velocity normally required even in the surf zone to predict is the instantaneous sediment transport rate from which the net transport rate can be computed.

In this paper, the numerical model of Kobayashi et al. (1987) developed for predicting the waterline oscillation on the rough impermeable slope of a coastal structure is slightly modified and applied to predict the swash oscillation on a natural beach. Kobayashi and Creenwald (1986,1988) showed that the numerical model could predict the measured temporal variations of hydrodynamic quantities on a 1:3 gravel slope with an impermeable base. Moreover, Kobayashi and Watson (1987) showed that the numerical model could also be applied to coastal structures with smooth slopes by adjusting the friction factor associated with the slope roughness. Kobayashi and Wurjanto (1988) extended the numerical model to predict wave overtopping over coastal structures. These applications of the numerical model to coastal structures were limited to uniform slopes of 1:5 or steeper as well as composite slopes. On the other hand, Kobayashi et al. (1988) modified the numerical model slightly to predict the wave transformation in the surf and swash zones on gentle slopes as well as the wave reflection and swash oscillation on

¹Assoc. Prof., Dept. of Civil Engrg., Univ. of Delaware, Newark, DE 19716.

²Civil Engineer, Planning Div., U.S. Army Corps of Engineers, Baltimore District, P.O. Box 1715, Baltimore, MD 21203.

³Crad. Student, Dept. of Civil Engrg., Univ. of Delaware, Newark, DE 19716.

relatively steep beaches. The slight modification was related to the effect of the wave-induced current on the seaward boundary condition used in the numerical model, which influenced the computed mean water level on gentle slopes. The modified numerical model was compared with small-scale test data for monochromatic waves spilling on gentle slopes. The comparison included the comprehensive test results for a 1:40 smooth slope presented by Stive (1980) and Stive and Wind (1982) as well as the undertow measurement for a 1:34.25 smooth slope performed by Hansen and Svendsen (1984). The numerical model was shown to be capable of predicting the development of the wave profile asymmetry about the vertical axis from the symmetric cnoidal wave profile outside the breakpoint to the sawtooth profile in the inner The computed shoreline oscillation on the gentle slope surf zone. showed the dominance of the setup over the swash in accordance with the empirical formulas proposed by Battjes (1974). As a whole, the numerical model was in good agreement with the gentle slope data except that the numerical model based on the finite-amplitude shallowwater equations predicts the depth-averaged velocity only and can not predict shoaling without wave breaking over the horizontal distance which is large relative to the wavelength. In order to take the seaward boundary location far seaward of the breakpoint, the numerical model would need to be matched with a numerical model based on the Boussinesq equations for a sloping bottom (Peregrine, 1967) such as the time domain model of Abbott et al. (1984) and the frequency domain model of Freilich and Guza (1984). In addition, Kobayashi et al. (1988) compared the modified numerical model with the wave reflection and swash excursion measurements for monochromatic waves plunging and surging on a 1:8.14 slope described by Guza and Bowen (1976) and Guza et al. (1984). The agreement between the model and the data was only qualitative probably because the wave reflection data was obtained on the basis of linear standing wave theory and the visual measurements of swash excursion on the relatively steep slope were difficult to define quantitatively. Kobayashi et al. (1988) also conducted smallscale tests for monochromatic and transient grouped waves on a 1:8 slope with and without an idealized nearshore bar at the toe of the 1:8 slope. The numerical model was shown to be capable of predicting the measured shoreline oscillations fairly well.

In the following, the numerical model used by Kobayashi et al. (1988) is described concisely and compared with the field data on swash oscillations on a moderately steep beach with a nearshore bar given by Holman and Sallenger (1985). As a first attempt, incident random waves are approximated by monochromatic waves, although any incident wave train in the time domain could be specified as input at the seaward boundary of the numerical model. This monochromatic approximation may be reasonable for the swash oscillation in the incident frequency band but excludes the swash oscillation in the infragravity frequency band which was not negligible for the field data. The sediment transport mechanics in the swash zone on a natural beach are discussed only briefly at the end of this paper.

ONE-DIMENSIONAL UNSTEADY NUMERICAL FLOW MODEL

Under the assumptions of alongshore uniformity and normally incident waves, the finite-amplitude shallow-water equations for an impermeable beach of arbitrary geometry are expressed as (Kobayashi et al., 1988)

 $\frac{\partial \mathbf{h'}}{\partial \mathbf{t'}} + \frac{\partial}{\partial \mathbf{x'}} (\mathbf{h'u'}) = 0$

(1)

$$\frac{\partial}{\partial t'} (h'u') + \frac{\partial}{\partial x'} (h'u') = -gh' \frac{\partial \eta'}{\partial x'} - \frac{1}{2} f' |u'|u'$$
(2)

where t'-time; x'-horizontal coordinate taken to be positive in the landward direction with x'=0 at the seaward boundary of the numerical model; h'=instantaneous water depth; u'=instantaneous depth-averaged horizontal velocity; g=gravitational acceleration; η' =instantaneous free surface elevation above the still water level (SWL); and f'=bottom friction factor which is assumed constant. The prime indicates the dimensional variables which are normalized in the following. The vertical coordinate z' is taken to be positive upward with z'=0 at SWL. The arbitrary beach geometry is specified by d'_=water depth below SWL at x'=0 and θ' =local angle of the bed varying with respect to x'>0. Denoting the reference wave height and period by H'_r and T'_r, respectively, which are assumed to be given, the following dimensionless variables are introduced:

$$t = \frac{t'}{T'_{r}} ; \qquad x = \frac{x'}{T'_{r}/gH'_{r}} ; \qquad u = \frac{u'}{\sqrt{gH'_{r}}}$$
(3)

$$z = \frac{z'}{H'_r} ; \qquad h = \frac{h'}{H'_r} ; \qquad \eta = \frac{\eta'}{H'_r} ; \qquad d_t = \frac{d_t^2}{H'_r}$$
(4)

$$\sigma = T'_{r} \int_{H'_{r}}^{\underline{g}} ; \quad \theta = \sigma \tan \theta' ; \quad f = \frac{1}{2} \sigma f'$$
 (5)

In terms of the normalized coordinate system, the bed is located at

$$z = \int_{0}^{x} \theta dx - d_{t} \quad ; \quad \text{for } x \ge 0$$
 (6)

Substitution of Eqs. 3-5 into Eqs. 1 and 2 yields

$$\frac{\partial h}{\partial t} + \frac{\partial m}{\partial x} = 0 \tag{7}$$

$$\frac{\partial m}{\partial t} + \frac{\partial}{\partial x} \left(m h^{-} + \frac{1}{2} h \right) = -\theta h - f |u| u$$
(8)

in which m=uh is the normalized volume flux per unit width.

Eqs. 7 and 8 expressed in the conservation-law form of the mass and momentum equations except for the two terms on the right hand side of Eq. 8 are solved in the time domain using the explicit dissipative Lax-Wendroff finite difference method based on a finite-difference grid of constant space size Δx and constant time step Δt as explained by Kobayashi et al. (1987). The initial time t=0 for the computation marching forward in time is taken to be the time when the incident wave train specified as input arrives at the seaward boundary, x=0, and no wave action is present in the computation domain $x \ge 0$. The landward boundary on the beach is located at the moving shoreline where the water depth is essentially zero. For the computation, the shoreline is defined as the location where h equals an infinitesimal value δ . The shoreline oscillation is computed using the predictorcorrector-smoothing procedure explained by Kobayashi et al. (1987). The seaward boundary at x=0 is taken to be located seaward of the breakpoint where the flow at x=0 can be assumed to be subcritical and satisfy the condition $u < \sqrt{h}$. Expressing Eqs. 7 and 8 in the

characteristic forms, the equation for the characteristics, β =(-u+2 \sqrt{h}), advancing seaward at x=0 is given by Kobayashi et al. (1987)

$$\frac{\partial \beta}{\partial t} + (u - \sqrt{h}) \frac{\partial \beta}{\partial x} = \theta + \frac{f|u|u}{h} \qquad ; \qquad \text{along } \frac{dx}{dt} = u - \sqrt{h} \qquad (9)$$

Eq. 9 is discretized using a simple first-order finite difference to obtain the value of $\beta = (-u+2\sqrt{h})$ (Kobayashi et al., 1987). In addition, the total water depth at the seaward boundary is expressed in the form

$$h = d_t + \eta_i(t) + \eta_r(t)$$
; at $x = 0$ (10)

in which η_i and η_r are the free surface variations with respect to t at x=0 normalized by the reference wave height H'_r . The incident wave train seaward of the breakpoint is specified by prescribing the variation of η_i with respect to t≥0. The term $\eta_r(t)$ in Eq. 10 accounts for the difference between the actual value $\eta_{-}(\eta_i+\eta_r)$ at x=0 and the prescribed value η_i . For reflective slopes such as coastal structures, $\eta_r(t)$ may be regarded as the normalized free surface variation associated with the reflected wave train at x=0 (Kobayashi et al., 1987). For dissipative beaches, incident wave reflection may be negligible but $\eta_r(t)$ accounts for the secondary effects excluded from the prescribed variation of $\eta_i(t)$. Kobayashi et al. (1988) used the following approximate expression of $\eta_r(t)$ in terms of the value of β at x=0 computed using Eq. 9:

$$\eta_{\rm r}(t) \simeq \frac{1}{2} \sqrt{d_t} \beta(t) - d_t - C_t$$
; at x = 0 (11)

with
$$C_t = -\frac{1}{2}\sqrt{d_t} \,\overline{u}_t$$
 (12)

where \bar{u}_t =value of the time-averaged horizontal velocity \bar{u} at x=0. Substitution of Eq. 11 into Eq. 10 yields the value of h at x=0 for given $\eta_1(t)$ and estimated C_t . The value of u at x=0 is then obtained from u=(2 $\sqrt{h}-\beta$) at x=0. The nonlinear correction term C_t associated with the time-averaged velocity \bar{u}_t was not included in the numerical model developed for coastal structures by Kobayashi et al. (1987). This term was shown by Kobayashi et al. (1988) to improve the prediction of wave set-down and setup on a gentle slope.

The time-averaged mass and momentum equations corresponding to Eqs. 7 and 8 can be expressed as

$$\overline{\mathbf{m}} = \overline{\mathbf{h}\mathbf{u}} = 0 \tag{13}$$

$$\frac{\mathrm{d}}{\mathrm{dx}}\left[\overline{\mathrm{hu}^2} + \frac{1}{2}\overline{(\eta - \overline{\eta})^2}\right] = -\overline{\mathrm{h}} \frac{\mathrm{d}\overline{\eta}}{\mathrm{dx}} - f \overline{|\mathrm{u}|\mathrm{u}}$$
(14)

where the overbar denotes time averaging and $\overline{\eta}$ is the vertical difference between the mean and still water levels. Use is made of the condition of no flux into the assumed impermeable beach to derive Eq. 13. The left hand side of Eq. 14 is the normalized gradient of the cross-shore radiation stress (e.g., Svendsen et al., 1987) under the assumptions of vertical uniformity and hydrostatic pressure. In this paper, the computed temporal variations of h and u at given location are used to compute the cross-shore variations of $\overline{\eta}$ and u without using Eqs. 13 and 14. Rearranging Eq. 13, the time-averaged horizontal velocity \overline{u} can be expressed as

$$\overline{\mathbf{u}} = - \overline{(\eta - \overline{\eta})(\mathbf{u} - \overline{\mathbf{u}})} \quad (\overline{\mathbf{h}})^{-1} \tag{15}$$

For gentle slopes with little wave reflection, $(\eta-\overline{\eta})$ and $(u-\overline{u})$ are expected to be in phase, resulting in $\overline{u}<0$ from Eq. 15. The computed seaward velocity \overline{u} was found to be smaller than the undertow measured below the wave trough since the numerical model does not account for the vertical variation of the time-averaged horizontal velocity (Kobayashi et al., 1988). An approximate value of \overline{u}_t may be found using Eq. 15 with the assumption of incident monochromatic linear long wave at the seaward boundary where the wave height and period are given by H' and T', respectively. Under this assumption, $(\eta-\overline{\eta}) \approx$ $(K_s/2) \cos(2\pi t), (u-\overline{u}) \approx (\eta-\overline{\eta})/\sqrt{d_t}$ and $\overline{h} \approx d_t$ at x=0, where $K_s=H'/H'_r$ and T'=T'_r is assumed. For gentle slopes with little wave reflection, \overline{u}_t and C_t may hence be approximated by

$$\overline{u}_{t} \simeq - K_{s}^{2} (8d_{t}^{3/2})^{-1}; \qquad C_{t} \simeq K_{s}^{2} (16d_{t})^{-1}$$
(16)

It should be mentioned that Kobayashi et al. (1988) used $K_s=1$ since the reference wave height H'_r was taken to be the wave height H' at the seaward boundary. For steep slopes with significant wave reflection for which η_r is on the order of unity, it might be more reasonable to assume that $u_t \simeq 0$ and $C_t \simeq 0$, but the effect of C_t on η_r in Eq. 11 is generally very small. For the previous comparisons made for coastal structures by Kobayashi et al. (1987), $d_t \ge 3$ and $K_s=1$, so that $C_t \le 0.02$. For gentle slopes, it is necessary to choose a smaller value of d_t so that the seaward boundary is not located too far seaward of the breakpoint (Kobayashi et al., 1988).

COMPARISON WITH SWASH OSCILLATIONS MEASURED ON A BEACH

The numerical model is compared with the wave setup and swash statistics on a moderately steep beach given by Holman and Sallenger (1985). The field data were collected over a 3-week period in October, 1982 at the Army Corps of Engineers Field Research Facility located at Duck, North Carolina. Fig. 1 shows the beach profile on October 26, 1982 which was given as an example profile in their paper.

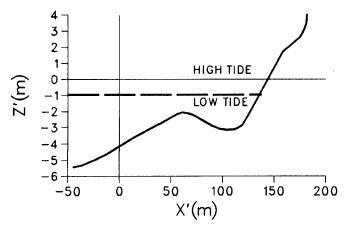


Fig. 1. Beach Profile with High and Low Tides

The slope angle θ'_{f} of the steep foreshore composed of coarse sand (mean size of 1-2 mm) varied between 5° and 9° (Sallenger et al., 1985). The position and height of the single bar shown in Fig. 1

varied in response to storm events, while the bar morphology varied from linear to crescentric. The incident wave data were collected from a wave-rider buoy in approximately 20-m depth. The significant wave height and peak period based on the measured spectra were given by Holman and Sallenger (1985) and are used herein as the reference wave height H'_r and period T'_r used for the normalization in Eqs. 3-5. During the experiment, $H'_{+} = 0.4-4.0m$ and $T'_{+} = 6-16s$. No information on wave direction was given in their paper. The tide data was provided by a tide gauge located outside the surf zone for all but the largest storm. The measured tidal range was -0.35m to 1.10m relative to the datum. The swash oscillation data were collected by using longshore-looking time-lapse photography together with large markers. A frame was shot every second for a total run length of 35 min. Sixty-one films were digitized, most at two longshore locations 100 and 150 m from the camera, but some films with apparent longshore variability were digitized more intensively. The digitized time series of the shoreline oscillation for each run were transformed to the vertical component from which the mean and the standard deviation The tidal elevation was subtracted from the $\sigma_{\rm c}$ were calculated. calculated mean to find the setup, whereas the significant swash height was taken as $4\sigma_s$. The total runup was defined as the sum of the setup and $2\sigma_{\rm s}$. The setup and swash statistics were calculated for a total of 154 time series. Holman and Sallenger (1985) normalized the setup, swash height and total runup by the significant wave height H_{τ}^{\prime} and plotted the normalized setup, swash height and total runup as a function of the surf similarity parameter defined as

$$\xi = \frac{\sigma \tan\theta'_{f}}{\sqrt{2\pi}} = T'_{f} \left(\frac{g}{2\pi H'_{f}}\right)^{1/2} \tan\theta'_{f}$$
(17)

where σ is defined in Eq. 5 and the foreshore slope $\tan\theta'_{f}$ ranged from 0.09 to 0.16 for the range of θ'_{f} -5°-9° indicated by Sallenger et al. (1985). In order to reduce the scatter of the plotted data points, the data were split into three sections corresponding to low, mid and high tides. The cutoff tidal elevations were arbitrarily taken as 0.25 and 0.70 m of the measured tidal range of -0.35 to 1.10 m. The mid and high tide data were similar, while the low tide data showed some influence of the single bar depicted in Fig. 1. As a result, the mid tide data is excluded from the following comparison.

The one-dimensional numerical model is based on the assumption of alongshore uniformity and normally incident waves. The field data may have satisfied these assumptions approximately near the shoreline when the bar morphology was linear and edge waves were absent. Sallenger and Holman (1987) analyzed the measured cross-shore flow during a storm in October, 1982. Prior to the storm, the bar was reasonably linear and shore parallel. The bar became increasingly crescentric when the wave heights were decreasing following the storm. The measured infragravity band spectra had characteristics consistent with either high-mode edge waves or standing (leaky) waves. As a result, the basic assumptions may not have been satisfied always, but the numerical model may still be applied to predict the trend of the scattered data points plotted by Holman and Sallenger (1985) since the assumptions of alongshore uniformity and normally incident waves must have been satisfied for some of the plotted data points. For the following computation, the beach profile shown in Fig. 1 is used as a typical profile neglecting the beach profile changes. The representative tidal elevations relative to the datum for the high and low tide data are simply taken as 0.90m and -0.05m, respectively. The vertical coordinate z' with z'=0 at SWL shown in Fig. 1 is that assumed for the high tide. The seaward boundary of the numerical model located at x'=0 in Fig. 1 is taken to be sufficiently seaward of the bar so that the normalized incident wave profile $\eta_1(t)$ at x'=0 may be specified as input using an appropriate wave theory for an essentially horizontal seabed. The water depth below SWL at x'=0 in Fig. 1 is dt=4.15m for the high tide and dt=3.20m for the low tide. As a first attempt, the incident random waves measured in approximately 20-m depth are assumed to be represented by the monochromatic wave whose height and period are the significant wave height H'_r and the spectral peak period T'_r used by Holman and Sallenger (1985) to plot their data. Table 1 shows five different cases selected for the subsequent computation to represent the range of the wave conditions associated with the field data except that cases with larger wave heights are excluded to avoid wave breaking seaward of the selected seaward boundary location. The surf similarity parameter ξ

TABLE 1. Five Different Wave Conditions Used for Computation

Case	H _r (m)	T _r (s)	σ	Ę
1	2.0	7	15.5	0.73
2	0.9	7	23.1	1.09
3	1.6	12	29.7	1.40
4	0.8	11	38.5	1.82
5	0.8	14	49.0	2.31

is defined in Eq. 17 where the foreshore slope $\tan\theta'_{\rm f}=0.118$ at the still water shoreline for the beach profile shown in Fig. 1. The range of ξ for the selected cases corresponds to that for the field data. For each case, a shoaling analysis is performed to find the wave height H' at x'=0 where the water depth d'_t below SWL is taken as 4.15 m for the high tide and 3.20 m for the low tide. In this paper, the shoaling analysis and the specification of the normalized incident wave profile $\eta_{\rm i}(t)$ for t>0 are made using cnoidal wave theory for Ur>26 and Stokes second-order wave theory for Ur<26 in which Ur=Ursell parameter at x'=0 defined below (Svendsen and Brink-Kjaer, 1972). Table 2 summarizes the estimated monochromatic wave characteristics at

TABLE 2. Wave Characteristics at Seaward Boundary for High and Low Tides

Case	d _t	K _s	L	U _r	r
H1	2.08	1.03	11.1	61	0.02
H2	4.61	1.07	10.1	24	0.02
H3	2.59	1.58	21.5	283	0.05
H4	5.19	1.35	17.4	79	0.11
H5	5.19	1.58	23.0	161	0.17
L1	1.60	1.16	14.0	141	0.02
L2	3.56	1.10	12.2	46	0.02
L3	2.00	1.93	27.6	734	0.04
L4	4.00	1.56	21.0	171	0.07
L5	4.00	1.85	27.9	359	0.10

the seaward boundary of the numerical model for the five cases listed in Table 1, where the capital letters H and L indicate the high and low tides, respectively. In Table 2, d_{t} = $d_{t}^{\prime}/H_{r}^{\prime}$ and $K_{s},$ L and U_{r} are defined as

$$K_{s} = \frac{H'}{H'_{r}} ; \qquad L = \frac{L'}{d'_{t}} ; \qquad U_{r} = \frac{H'(L')}{(d'_{t})} = \frac{K_{s}L}{d_{t}}$$
(18)

where L'-wavelength at x'=0. The assumption of finite-amplitude shallow-water waves in the computation domain x'≥0 may be appropriate since L>>1 and U_x>>1. Table 2 also lists the computed reflection coefficient r for each case. The value of r is estimated as the height of the computed periodic variation of $\eta_r(t)$ divided by K_s, as will be explained later, where the period and height of the periodic variation of $\eta_1(t)$ are equal to unity and K_s, respectively. The computed reflection coefficient r increases with the increase of the surf similarity parameter ξ . This trend is similar to that for coastal structures (Kobayashi and Watson, 1987). However, the value of r in Table 2 with the corresponding value of ξ in Table 1 is smaller than that based on the empirical formula, r=(0.1 ξ)≤1, for smooth plane slopes proposed by Battjes (1974) even if H'-K_sH'_r is used instead of H'_r in Eq. 17 to reduce the value of ξ for each case.

For the subsequent computation, use is made of approximately 400 nodes in the computation domain $x' \ge 0$ in Fig. 1 with the dimensional space size $\Delta x' \simeq 0.46m$ between the two adjacent nodes. Correspondingly, the dimensionless space size of the finite difference grid is in the range of $\Delta x=0.0097-0.022$ for the ten cases listed in Table 2. The number of time steps over one normalized wave period of unity is taken as $(\Delta t)^2 = 4000$ except that $(\Delta t)^2 = 5000$ is used for Case L2 due to numerical instability. The computational shoreline is defined by h= δ =0.002 since the increase of this value from δ =0.001 used for smooth steep slopes (Kobayashi and Watson, 1987) tends to improve the numerical stability in the vicinity of the computational shoreline. The measured shoreline oscillation is defined by the physical water depth h'= δ_1 in which δ_1 ' ≈ 0.5 cm for the photography technique used by Holman and Sallenger (1985) and $\delta'_{r}=3.0$ cm for the dual-resistance wire sensor used by Guza and Thornton (1982) whose data are also included in the following comparison. For $H'_r=0.8-2.0$ m as shown in Table 1, $\delta_{r} = (\delta_{r}^{\prime}/H_{r}^{\prime}) > \delta = 0.002$. The numerical damping coefficients for reducing high frequency numerical oscillations at the rear of breaking wave crests are taken as two for gentle slopes (Kobayashi and DeSilva, 1987; Kobayashi et al., 1988). The bottom friction factor f' is tentatively assumed to be f'=0.05 on the basis of the limited calibration made by Kobayashi and Watson (1987) for small-scale smooth slopes without beach sand, neglecting the scale effects and the effects of moving sediment particles on f' (Kobayashi and Seo, 1985). The previous sensitivity analyses performed by Kobayashi et al. (1987) indicated that the computed results should not be very sensitive to the value of f'.

The computed results for the ten cases listed in Table 2 are given in the thesis of Strzelecki (1988). The computed results for Case H3 are presented as an example in the following. Fig. 2 shows the periodic cnoidal wave profile $\eta_1(t)$ specified at x=0 and the temporal variation of $\eta_{T}(t)$ computed using Eq. 11 with Eq. 16. The normalized wave period is unity. The detailed variation of $\eta_{T}(t)$ is shown in Fig. 3. The depression of η_{T} during the transition period 0st \leq 5 appears to be related to the depression of the mean water level under large waves (Longuet-Higgins and Stewart, 1962) since the incident wave train initially propagates into the region of no wave action. The temporal variation of $\eta_{T}(t)$ for $t \geq 10$ consists of steady and oscillatory components. The steady component is the wave set-down

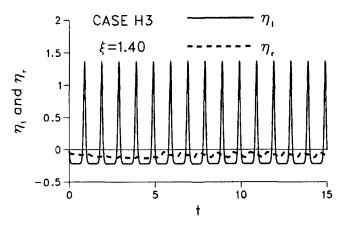


Fig. 2. Specified $\eta_i(t)$ and Computed $\eta_r(t)$ at Seaward Boundary

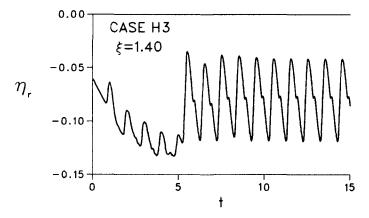


Fig. 3. Detailed Variation of $\eta_{r}(t)$ at Seaward Boundary

 $\overline{\eta}=\overline{\eta_r}$ at x=0 since $\overline{\eta_1}=0$ for the assumed cnoidal wave profile. oscillatory component is associated with the reflected wave. The The reflection coefficient r listed in Table 2 is taken as the height of this oscillatory component divided by the height of $\eta_i(t)$, that is, Ks. Fig. 4 shows the computed shoreline oscillations corresponding to the water depth $\delta'_r=0.5$ and 3cm plotted in the form of the normalized vertical elevation Z_r as a function of t. During wave downrush, the shoreline location is sensitive to the water depth δ_{r}' used to define its location since a thin layer of water remains on the relatively steep foreshore during wave downrush (Kobayashi et al., 1988). After the initial transient oscillation, the temporal variation of Z_r for t \gtrsim 6 is composed of steady and oscillatory components. The steady component is the normalized setup on the foreshore denoted by \overline{Z}_{r} , while the oscillatory component is the normalized swash about the setup level. The maximum and minimum values of $Z_r(t)$ after the establishment of periodicity are denoted by R and R_d in which R and R_d are the run-up and run-down normalized by the reference wave height H'_r , respectively. The value of (R-R_d) is the

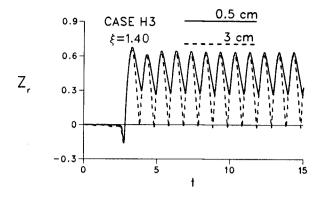


Fig. 4. Shoreline Oscillations for $\delta'_r = 0.5$ and 3 cm

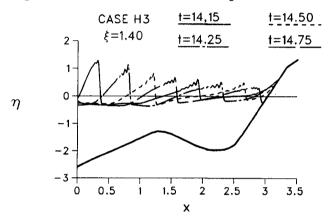


Fig. 5. Free Surface Variations During One Wave Period

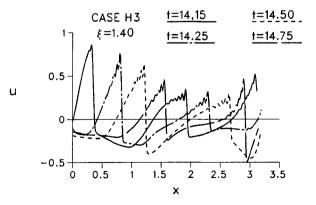
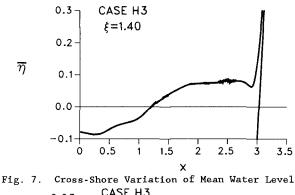


Fig. 6. Horizontal Velocity Variations During One Wave Period

normalized swash height. The computed values of \overline{Z}_r , R and R_d for given δ'_r are obtained using the computed variation of $Z_r(t)$ during $t_p \le t \le (t_p+1)$. For Case H3, $t_p=14$ is used since the periodicity is definitely established before t=14. $t_p=14$ is also found to be adequate for the other cases except for Cases L1 and L2 for which $t_p=24$ is used to ensure the definite periodicity. Figs. 5 and 6 show the computed cross-shore variations of η and u at t=14, 14.25, 14.5, 14.75 and 15, respectively. The normalized beach profile given by Eq. 6 is also shown in Fig. 5. The computed variations of η and u at t=14 and 15 are identical. The effects of the bar on the variations of η and u landward of the bar are apparent in Figs. 5 and 6. Figs. 7 and 8 show the computed cross-shore variations of the time-averaged free surface elevation η above SWL and the time-averaged horizontal velocity \overline{u} , respectively, where the time averaging is performed for



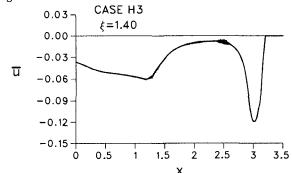


Fig. 8. Cross-Shore Variation of Mean Horizontal Velocity

 $t_p \leq t \leq (t_p+1)$. The effects of the bar on the setup and mean velocity landward of the bar are apparent in these figures. Fig. 7 indicates that the mean water level on the steep foreshore will be affected by the large swash oscillation. Fig. 8 suggests that the bar may modify the cross-shore variation of the undertow noticeably, although \bar{u} is not the same as the undertow (Kobayashi et al., 1988).

The values of \overline{Z}_r , R and (R-R_d) for δ'_r =0.5 and 3 cm computed for each of the ten cases in Table 2 are plotted in Fig. 9 as a function of the surf similarity parameters ξ for the high and low tides. The data points in Fig. 9 are read from the figures given in Holman and Sallenger (1985) where \overline{Z}_r , R and (R-R_d) are assumed to be the same as the nondimensional setup, total runup and significant swash height

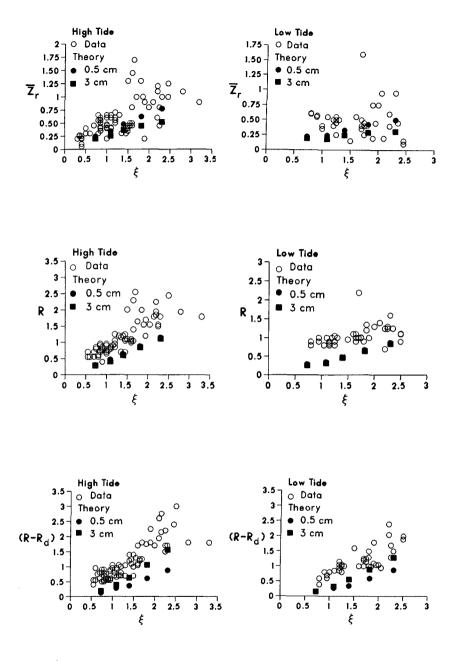


Fig. 9. Comparisons of Measured and Computed Setup, Run-up and Swash Height for High and Low Tides

calculated from the mean and standard deviation of the measured time series of the shoreline location with $\delta'_r \simeq 0.5$ cm on the foreshore slope of approximately 0.1. The data points for the high tide included those measured by Guza and Thornton (1982) on a beach slope of approximately 0.023 using a wire sensor with $\delta_L^*=3$ cm. These data points were in the region of $\xi < 1$. The differences between these two data sets were discussed by Guza et al. (1984). The computed results for $\delta'_{\rm T}=0.5$ and 3 cm suggest that the two measuring techniques will yield large differences in $(R-R_d)$ and \overline{Z}_r for $\xi \ge 2$. Intercalibration of the two techniques on a low-slope beach indicated that the film technique registered a slightly higher mean and a 35% larger standard deviation than the wire sensor. The intercalibration results are consistent with the computed results for \overline{Z}_r but opposite to the computed results for (R-R_d). Considering the subjective interpretation of run-down of the films especially for large values of ξ , it appears to be difficult to specify an appropriate value of δ'_{T} for the film technique unlike the wire sensor with a specific value of δ_{r}^{\prime} . The effects of permeability neglected in the numerical model may not be negligible on the foreshore slope composed of coarse sand (Packwood, 1983). However, the premeability effects should reduce the computed values of R and $(R-R_d)$. The underestimation of R and $(R-R_d)$ by the numerical model is expected to be caused mainly by the monochromatic wave approximation which may be reasonable only for the swash oscillation in the incident frequency band. The computed values of $(R-R_d)$ with $\delta'_{L}=3$ cm for the high and low tides are plotted on Fig. 10(a) of Holman and Sallenger (1985) which

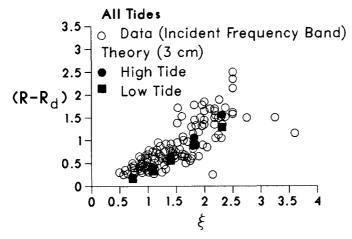


Fig. 10. Comparison with Swash Height in Incident Frequency Band

showed the nondimensional significant swash height in the incident frequency band (frequency ≥ 0.05 Hz) for all tides. The computed points with δ'_{T} -3 cm follow the trend of the scattered data points well as shown in Fig. 10. However, the computed points with δ'_{T} -0.5 cm, which are not shown in Fig. 10, are less than those shown in Fig. 10. Figs. 9 and 10 imply that the monochromatic approximation without regard to the swash oscillation in the infragravity frequency band will underestimate the swash height and run-up even on the moderately steep foreshore. Extension of the numerical model to random waves is

definitely required, although wave group statistics in shallow water are not well known (Elgar et al., 1984).

SEDIMENT TRANSPORT IN SWASH ZONE

Kobayashi (1988) assembled and synthesized recent publications which might contribute to the improvement of our quantitative capabilities for predicting shoreline changes due to the cross-shore sediment transport in the surf and swash zones on beaches. The comparisons shown above suggest that an accurate prediction of the swash oscillation including the effects of random waves and actual beach profiles is essential for predicting the resulting sediment movement in the swash zone. It should be stated that purely empirical models for beach and dune erosion might work reasonably well for highly erosive storm events if storm surge is more important than Nevertheless, an improved understanding of the hydrodynamics swash and resulting sediment movement in the swash zone is required for better establishing the landward boundary condition for such an erosion model as well as for predicting accretion and berm building. Even for laboratory data with monochromatic waves, it appears to be difficult to explain the detailed processes of berm building. Kobayashi and DeSilva (1987) applied a Lagrangian sediment transport model to predict the movement of individual bedload particles in the swash zone under monochromatic wave action. The Lagrangian model, which did not include the correction term Ct in Eq. 11, was found to explain observed erosion and bar formation of an initially uniform sand slope but could not predict observed accretion and berm building. The major reason appeared to be the large water velocity during the wave downrush predicted by the numerical model which neglected the permeability effects.

ACKNOWLEDCEMENT

This work is a result of research sponsored by NOAA Office of Sea Grant, Department of Commerce, under Crant No. NA85AA-D-SG033 (Project No. R/OE-3). The U.S. Government is authorized to produce and distribute reprints for government purposes notwithstanding any copyright notation that may appear herein.

REFERENCES

- Abbott, M.B., McCowan, A.D. and Warren, I.R. (1984). "Accuracy of short-wave numerical models." <u>J. Hydraulic Engrg.</u>, ASCE, 110(10), 1287-1301.
- Battjes, J.A. (1974). "Surf similarity." <u>Proc. 14th Coast. Engrg.</u> <u>Conf.</u>, ASCE, 466-480.
- Battjes, J.A. and Stive, M.J.F. (1985). "Calibration and verification of a dissipation model for random breaking waves." <u>J. Ceophys.</u> <u>Res.</u>, 90(C5), 9159-9167.

Elgar, S., Guza, R.T. and Seymour, R.J. (1984). "Croups of waves in shallow water." J. Ceophys. Res., 87(C3), 3623-3634.

- Freilich, M.H. and Cuza, R.T. (1984). "Nonlinear effects on shoaling surface gravity waves." <u>Philos. Trans. R. Soc. London</u>, Ser. A, 311, 1-41.
- De Vriend, H.J. and Stive, M.J.F. (1987). "Quasi-3D modelling of nearshore currents." <u>Coast, Engrg.</u>, 11, 565-601.
- Cuza, R.T. and Bowen, A.J. (1976). "Resonant interactions for waves breaking on a beach." <u>Proc. 15th_Coast. Engrg. Conf.</u>, ASCE, 560-579.
- Cuza, R.T. and Thornton, E.B. (1982). "Swash oscillations on a natural beach." <u>J. Geophys. Res.</u>, 87(Cl), 483-491.

- Cuza, R.T., Thornton, E.B. and Holman, R.A. (1984). "Swash on steep and shallow beaches." Proc. 19th Coast. Engrg. Conf., ASCE, 708-723.
- "A theoretical and Hansen, J.B. and Svendsen, I.A. (1984). experimental study of undertow." Proc. 19th Coast. Engrg. Conf., ASCE, 2246-2262.
- Holman, R.A. and Sallenger, A.H. (1985). "Setup and swash on a natural beach." J. Ceophys, Res., 90(C1), 945-953.
- Kobayashi, N. and Seo, S.N. (1985). "Fluid and sediment interaction on a plane bed." J. Hydraulic Engrg., ASCE, 111(6), 903-921.
- Kobayashi, N. and Creenwald, J.H. (1986). "Prediction of wave runup and riprap stability." Proc. 20th Coast. Engrg. Conf., ASCE, 1958-1971.
- Kobayashi, N., Otta, A.K. and Roy, I. (1987). "Wave reflection and runup on rough slopes." J. Wtrway. Port Coast. and Oc. Engrg., ASCE, 113(3), 282-298.
- Kobayashi, N. and Watson, K.D. (1987). "Wave reflection and runup on smooth slopes." Proc. Coast. Hydrodynamics, ASCE, 548-563.
- Kobayashi, N. and DeSilva, C.S. (1987). "Motion of sediment particles in swash zone." Proc. Coast. Hydrodynamics, ASCE, 715-730.
- Kobayashi, N. and Creenwald, J.H. (1988). "Waterline oscillation and riprap movement." J. Wtrway. Port Coast. and Oc. Engrg., ASCE, 114(3), 281-296.
- Kobayashi, N. (1988). "Review of wave transformation and cross-shore sediment transport processes in surf zones." J. Coast. Res., 4(3), (in press).
- Kobayashi, N. and Wurjanto, A. (1988). "Wave overtopping on coastal structures." J. Wtrway. Port Coast. and Oc. Engrg., ASCE (in press).
- N., DeSilva, C.S. and Watson, K.D. (1988). Kobayashi, "Wave transformation and swash oscillation on gentle and steep slopes." J. Ceophys. Res., (submitted).
- Longuet-Higgins, M.S. and Stewart, R.W. (1982). "Radiation stress and mass transport in gravity waves, with application to 'surf beats'." J. Fluid Mech., 13, 481-504.

Packwood, A.R. (1983). "The influence of beach porosity on wave uprush and backwash." Coast. Engrg., 7, 29-40.

Peregrine, D.H. (1967). "Long waves on a beach." J. Fluid Mech., 27, 815-827.

- Sallenger, A.H., Holman, R.A. and Birkemeier, W.A. (1985). "Storminduced response of a nearshore-bar system." Marine Ceology, 64, 237-257.
- Sallenger, A.H. and Holman, R.A. (1987). "Infragravity waves over a natural barred profile." J. Ceophys. Res., 92(C9), 9531-9540.
- Stive, M.J.F. (1980). "Velocity and pressure field of breakers." <u>Proc. 17th Coast. Engrg. Conf.</u>, ASCE, 547-566. "Velocity and pressure field of spilling
- Stive, M.J.F. and Wind, H.C. (1982). "A study of radiation stress and set-up in the nearshore region." <u>Coast. Engrg.</u> 6, 1-25.

Stive, M.J.R. (1986). "A model for cross-shore sediment transport." Proc. 20th Coast. Engrg. Conf., ASCE, 1550-1564. Strzelecki, M.S. (1988). "Wave setup and swash on a beach and wave

transmission over a nearshore bar." Will be presented to the University of Delaware in partial fulfillment of the requirements for the Master's degree in Civil Engineering. Svendsen, I.A. and Brink-Kjaer, O. (1972). "Shoaling of cnoidal

waves." Proc. 13th Coast. Engrg. Conf., ASCE, 365-383.

Svendsen, I.A., Schäffer, H.A. and Hansen, J.B. (1987). "The interaction between the undertow and the boundary layer flow on a beach." J. Ceophys. Res., 92(C11), 11845-11856.